

Supplementary Information

Cells in cell-culture media only experience negative dielectrophoresis

We present a plot below of the real part of the CM factor for a cell suspended in cell-culture media. For cell parameters, we used a membrane capacitance of $1.6 \mu\text{F}/\text{cm}^2$, membrane conductivity of $0.22 \text{ S}/\text{cm}^2$, cytoplasmic conductivity of $0.75 \text{ S}/\text{m}$ and cytoplasmic dielectric constant of 75. Medium conductivity is $1.5 \text{ S}/\text{m}$ and dielectric constant is 80. These values are all taken from Huang *et al* (*Biophysical Journal*, 1997, **73**, 1118). As can be seen from the graph, $\text{Re}(\text{CM})$ is always negative. Thus, cells in this medium always experience negative dielectrophoresis.

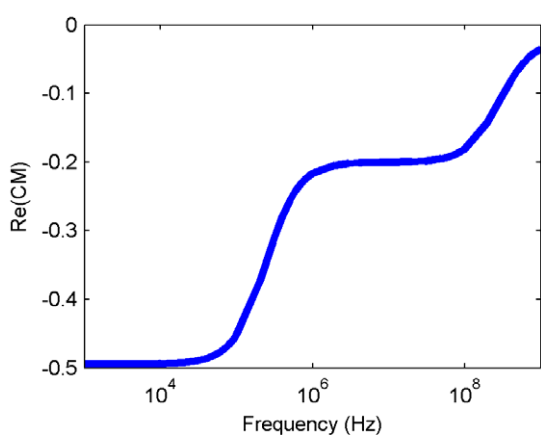


Figure S1. Graph of the real part of the CM factor for a cell suspended in cell-culture medium.

Cell-substrate friction/sticking and nDEP microwell design motivation

The figure below demonstrates the motivation for adding IDEs to our device. In earlier versions of the device without IDEs, large numbers of cells “stuck” to the substrate in the inter-trap region.

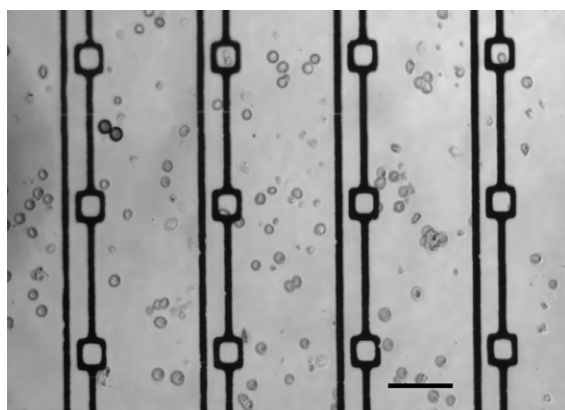


Figure S2. Image of NIH 3T3 fibroblasts patterned onto our earlier device which did not have IDEs, showing that significant numbers of cells stick to the Pyrex substrate outside the traps, which could not be removed with flow without also ejecting some trapped cells. The scale bar is $100 \mu\text{m}$.

We will now explain in detail why non-specific adhesion between cells and the substrate presented a significant challenge to patterning cells using nDEP. We refer to the force holding cells to the surface as friction since friction is defined as the force between two objects in contact that prevents their relative motion. Consider a trapped and an untrapped cell. The trapped cell experiences a DEP force F_{DEP} and a frictional force F_1 . The untrapped cell only experiences a frictional force F_2 (which may differ from F_1 as there is substantial variation in the frictional force). For successful patterning, we need the trapped cell to experience a significantly stronger force, so that the untrapped cell can be flowed away easily by applying F_{flow} such that $F_{untrapped} < F_{flow} < F_{trapped}$.

As we stated above, for this we need

$$\begin{aligned}F_{untrapped} &< F_{trapped} \\F_2 &< F_1 + F_{DEP} \\F_2 - F_1 &< F_{DEP} \\ \Delta F_{fric} &< F_{DEP}.\end{aligned}$$

Where $\Delta F_{fric} = F_2 - F_1$ is, more generally, the variation in the frictional force. However, we observe that this variation is typically around 10-15 pN while the DEP holding force at 1 V_{pp} is ~1 pN (from our modeling). As we do not wish to apply higher voltages due to cell health effects or EHD flows, we wished to find an alternate method to avoid cell-substrate interactions. Thus, we introduced IDEs to levitate untrapped cells and prevent contact between cells and the substrate outside of the trap region.

Effect of cell size and shape on the levitation height

For our simulations of the levitation height we assumed that the cell is a sphere of radius 5 μm. However, the levitation height is actually independent of the size of the sphere, since it is determined by the balance of DEP, gravitational and buoyancy forces. All these forces are directly proportional to the volume of the cell, thus the levitation height is size (volume) independent.

To address the question of how cell shape affects levitation height, we estimated the variation in levitation height due to variations in cell shape. Variations in shape only affect the Re(CM) in the expression for the DEP force. The CM factor for an ellipsoid can be written as

$$CM = \frac{1}{3} \frac{\epsilon_p - \epsilon_m}{n\epsilon_p + (1-n)\epsilon_m},$$

where ϵ_p and ϵ_m are the complex permittivities of the particle and medium respectively, and n is called the depolarization factor. (For a sphere, $n = 1/3$, which gives the familiar expression for CM factor of a sphere.) This expression is given in several texts, including Gimsa and Wachner (Biophys J, September 1999, p. 1316-1326, Vol. 77, No. 3). In the same work, they show that as the axis ratio varies from 1:1 for a sphere to 1:2 (say, or 2:1), the depolarization factor varies from 0.33 to ~0.2 (0.4). Correspondingly, the CM factor changes from 0.2 to 0.18 (0.21). We

repeated our simulation of the levitation height with these CM factors and found the variation in levitation height to be only $\sim 1 \mu\text{m}$.

In summary, neither the size nor the shape of the particle significantly affects levitation height of cells in our system.

Operating voltages

Several parameters govern the choice of operating voltages in our device – the DEP forces, cell health concerns due to heating ($V < 2.5 V_{pp}$) and induced transmembrane voltages ($V < 10 V_{pp}$), and the onset of convective flows. In fact, there are two choices of operating voltages to be made in our device. First, we pick a voltage to operate the array when loading cells. We pick this voltage to be $1 V_{pp}$ on account of two factors:

- The trap strength increases with voltage¹
- Above $1 V_{pp}$ however, the nDEP microwell becomes narrower and will no longer admit a cell (Fig.2, main manuscript).

Next, after the wells have been loaded, we must pick a voltage to apply to hold trapped cells and continue levitating untrapped cells while we flow them off the array. We picked this voltage also to be $1 V_{pp}$, though for a different reason. Above $1 V_{pp}$ we found that the EHD convective flow was quite strong, leading to fluid velocities of a few microns per second on the array. This caused bunching of cells in the center of the array, which then interacted strongly with each other, as well as the trapped cells, pulling them out of wells as they flowed over the array. We did however occasionally use the convective flow to load specific traps, as described elsewhere.

Temperature modeling and measurements

The steady-state heat conduction module in Femlab solves the equation

$$k\nabla \cdot T + Q = 0,$$

where k is the (isotropic) thermal conductivity
 T is the temperature, and
 Q is the heat source (or sink).

We set the temperature at all exterior surfaces to be 25°C . For our Pyrex substrate, we assumed the following values²: Thermal conductivity = 1.3 W/mK . Density = 2225 kg/m^3 .

Below we show our resistor-on-chip device which we used to validate our temperature modeling (Figure S3), as well a comparison of modeled and measured temperatures (Figure S4).

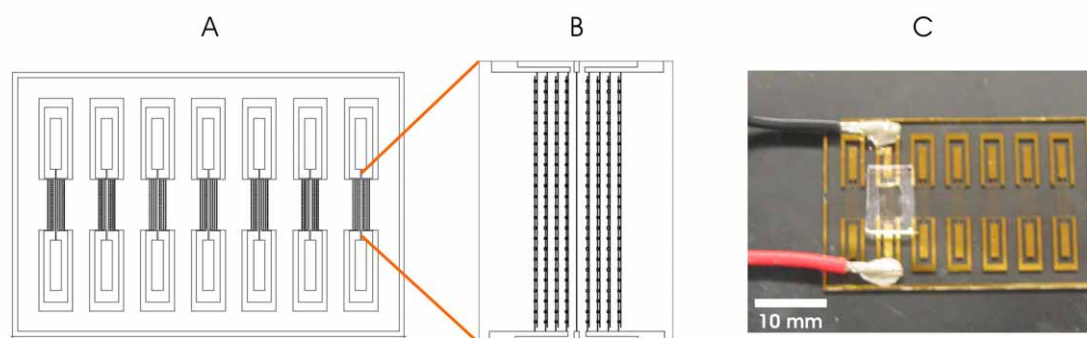


Figure S3. Resistor-on-chip (ROC) experiments. AutoCAD layout of: (A) the entire ROC electrode slide and (B) one ROC array, showing the ROC between eight rows of twenty-four DEP traps. (C) Actual experimental setup with electrode slide and flow chamber over the ROC array.

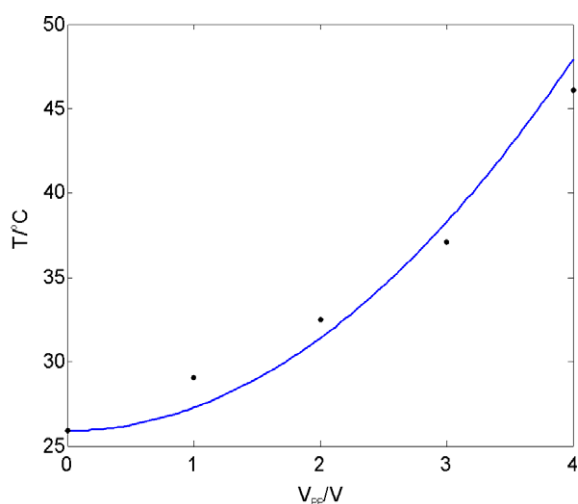


Figure S4. Validation of temperature modeling: Modeled temperatures (solid line) and measured temperatures (dots) versus voltage.

EHD voltage estimation

There are several ways that AC electric fields can produce fluid flow, most notably buoyancy-driven flows, electrothermal flows and AC electroosmosis. Buoyancy-driven flow occurs when Joule heating causes a gradient in density that sets up a convective flow. Electrothermal flows occur when Joule heating causes gradients in electrical properties that are then acted upon by electric fields, while AC electroosmosis describes coupling between double-layer charge and a transverse electric field. We believe that buoyancy-driven flow is the cause for the flows seen in our systems. AC electroosmosis is negligible at the high conductivities (1 S/m) and high frequencies (10 MHz) that we are using. The relative contributions of buoyancy versus electrothermal flows can be estimated using equation (51) in Castellanos *et al*³

$$\frac{F_b}{F_{et}} = \frac{(\partial\rho_m/\partial T)(\pi r)^3 g}{(1/\sigma)(\partial\sigma/\partial T)\epsilon V^2}.$$

For our system, at 1 V_{RMS}, the ratio of the buoyancy force to the electrothermal force F_b/F_{et} is almost 1000. So the flow is dominantly buoyancy-driven (Figure S5).

Finally, we show an analysis below that demonstrates that buoyancy-driven flow is consistent with our observations. The approximate fluid velocity v for such flows, due to an RMS potential V is given by³ (equation (52)),

$$v \sim 2 \cdot 10^{-2} \left(\frac{\partial\rho_m}{\partial T} \right) \frac{\sigma V^2 g r^2}{k\eta},$$

where σ is the electrical conductivity of the medium (1.5 S/m),
 g is the acceleration due to gravity (9.8 m/s²),
 r is the length scale, and
 k is the thermal conductivity of the medium (0.6 W/m/K)
 η is the dynamic viscosity (10⁻³ Pa.s).

$\left(\frac{\partial\rho_m}{\partial T} \right)$ represents the rate of change of density with temperature (0.25 kg/m³/K).

Values in parentheses represent values for the water-based medium (DMEM) used in our study.

From simulations, we observe that the length scale r is determined by the substrate thickness (i.e. $r \sim 1$ mm for our system). The convective flow is significant and useful for cell manipulation when $v = O(10 \mu\text{m/s})$. Substituting other values for in the equation above,

$$V_{RMS} \sim 0.3V$$

$$V_{pp} \sim 1V.$$

In our experiments we saw flows with approximately this velocity at around 3.0 V_{pp}. The qualitative agreement between the predicted and observed onset of flow further supports the hypothesis that the flows are indeed due to thermal buoyancy-induced convection.

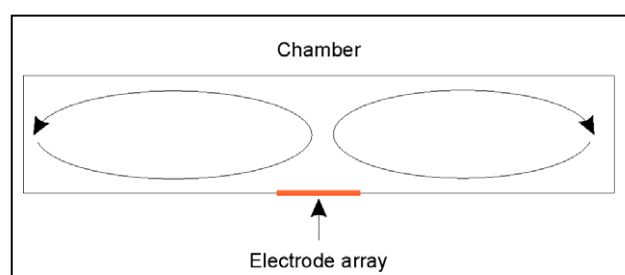


Figure S5. Schematic of convective flow in our device due to heating of the fluid by our electrode array.

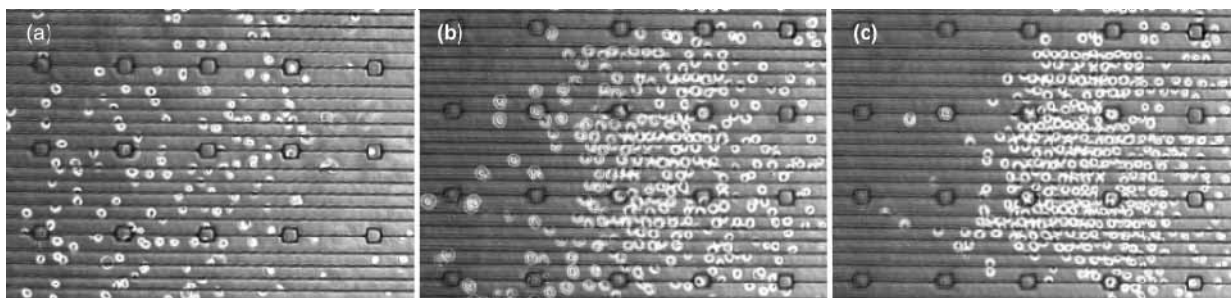


Figure S6. Concentration of cells using EHD convective flow by operating the electrode array at 2.5 Vpp.

Effects of low-conductivity (pDEP) media on ES cells

To assess the health effects of immersing cells in low conductivity media, we placed ABJ1 mouse ES cells in a sucrose solution for different lengths of time. After this, they were transferred to regular ES growth medium and expanded for five days. The plot below shows the reduction in cell number as a result of the exposure to this medium, as compared to high-conductivity medium (DMEM, plot corresponding to 0 minutes).

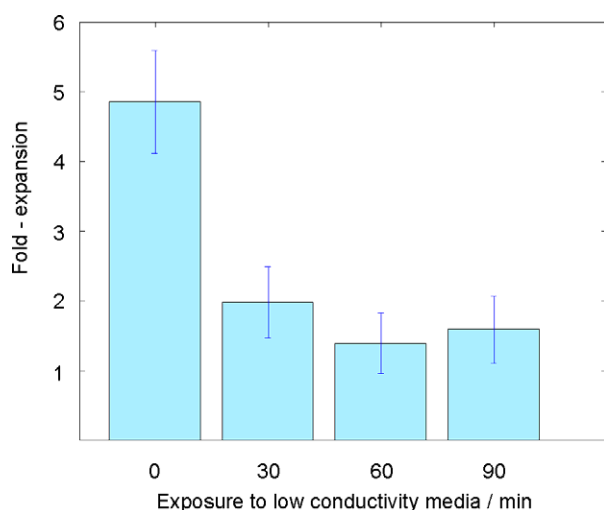


Figure S7. Plot of fold-expansion v/s length of exposure to low conductivity media for ABJ1 mESCs.

We cultured ABJ1 mESCs with a stably integrated GFP reporter for Oct-4 without feeders in ES media: DMEM (11960044, Invitrogen, Carlsbad, CA) supplemented with 15% ES-qualified fetal bovine serum (16141079, Invitrogen, Carlsbad, CA), 4 mM L-glutamine (25030081, Invitrogen, Carlsbad, CA), 1 mM non-essential amino acids, 50 U mL⁻¹ penicillin, 50 mg mL⁻¹ streptomycin (15140122, Invitrogen, Carlsbad, CA), 100 μM β-mercaptoethanol (M7522, Sigma, St Louis, MO), and 500 pM leukemia inhibitory factor (LIF, ESGRO, Chemicon,

Temecula, CA). We cultured cells directly on tissue-culture plastic (430639, Corning, Corning, NY) in a 37 °C humidified environment with 7.5% CO₂. For maintenance of mESCs, we fed cells daily and passaged every other day using 0.25% trypsin with 3.8 g L⁻¹ EDTA.4Na (25200056, Invitrogen, Carlsbad, CA) at a density of ~ 8 x 10⁴ cells cm⁻².

The pDEP media formulation was 20.5 mL of 50% sucrose solution, 1mL of ES serum, and 78.5 mL of ddH₂O.

Angle of flow

We briefly describe a “trick” we found useful for loading our device. It is natural to think of loading along the line of traps, which leads to a relatively small loading zone (Figure S8). I.e. a cell must land in this region to fill the trap in front of it. However, flowing at an angle allowed us to increase the loading zone by a factor of ~4, and correspondingly, to use a lower cell density. This mitigated the clumping of cells, and would also be useful when working with primary cells, sometimes available only in small numbers.

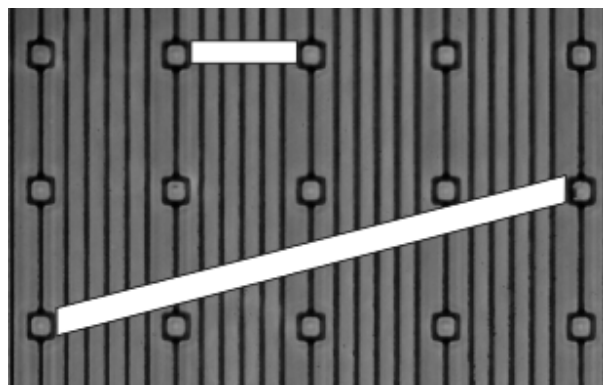


Figure S8. Flowing cells at an angle to the array increased the size of the loading zone (lower white parallelogram versus upper white rectangle) for each trap.

¹ A. Rosenthal and J. Voldman, *Biophysical Journal*, 2005, **88**, 2193.

² W. M. Rohsenow, J. P. Hartnett, and Y. I. Cho, 'Handbook of heat transfer', McGraw-Hill, 1998.

³ A. Castellanos, A. Ramos, A. Gonzalez, N. G. Green, and H. Morgan, *Journal of Physics D-Applied Physics*, 2003, **36**, 2584.